Available online at www.sciencedirect.com
SCIENCE DIRECT®
Journal of Solid State Chemistry 179 (2006) 968–973
JOURNAL OF SOLID STATE CHEMISTRY
www.elsevier.com/locate/jssc

Investigation of crystal structure and associated electronic structure of $Sr_6BP_5O_{20}$

Helmut Ehrenberg[a], Sonja Laubach[b], P.C. Schmidt[b,*], R. McSweeney[c], M. Knapp[a], K.C. Mishra[d]

[a]*Materials Science, Darmstadt University of Technology, Petersenstr. 23, 64287 Darmstadt, Germany*
[b]*Eduard-Zintl-Institut für Anorganische und Physikalische Chemie, Technische Universität Darmstadt, Petersenstr. 20, 64287 Darmstadt, Germany*
[c]*Precision Materials and Components, OSRAM SYLVANIA, Hawes Street, Towanda, PA 18848, USA*
[d]*Central Research, OSRAM SYLVANIA, Beverly, MA 01915, USA*

Received 5 August 2005; received in revised form 18 November 2005; accepted 11 December 2005
Available online 30 January 2006

Abstract

Strontium borophosphate phosphate ($Sr_6BP_5O_{20}$, SrBP), activated by divalent europium ions is a bluish-green phosphor emitting in a broad band with the emission peak near 480 nm. In this paper, we report the crystal structure of SrBP determined from an analysis of the X-ray diffraction pattern of a prismatic single crystal (size 60 μm × 50 μm × 40 μm). This crystal was chosen from undoped phosphor powder samples prepared for this purpose by solid-state reaction. SrBP is observed to crystallize in a body-centered tetragonal lattice with the lattice parameters $a = 9.7895(7)$ Å and $c = 19.032(3)$ Å, the associated space group being $I\bar{4}c2$ (space group 120). Using the structural data from this study, we have also calculated its electronic structure using the augmented spherical wave method and the local density approximation (LDA). We show the ordering of the electronic states by the density of states (DOS) and the partial DOS plots. The LDA gives a direct optical band gap at the Γ point of about 5 eV. The significance of the crystal structure and associated electronic structure is discussed with respect to maintenance of this phosphor in Hg-discharge lamps.

Keywords: Phosphor; Fluorescent lamps; CRI lamps; Host material; Strontium borophosphate phosphate; Divalent europium ions; Crystal structure; Single-crystal X-ray diffraction; Synchrotron powder diffraction; Thermal expansion; Electronic structure calculation; Band structure calculation

1. Introduction

Strontium borophosphate phosphate ($Sr_6BP_5O_{20}$, SrBP), activated by divalent europium ions is often used in fluorescent lamps for the purpose of improving their colour-rendering index (CRI). The divalent europium ions in this host emit in a broad band in the blue-green region of the spectrum with the emission peak near 480 nm due to $5d \rightarrow 4f$ transitions. With growing demand in the lighting industry for higher CRI lamps, this phosphor could find use in four-component phosphor coatings in Hg-discharge lamps. Unfortunately, it degrades faster than the usual tri-blend phosphor components, namely Y_2O_3:Eu^{3+} (red), $LaPO_4$:Tb^{3+}, and $BaMgAl_{10}O_{17}$:Eu^{2+} during lamp life, most likely due to interaction with Hg discharge. The exact nature of degradation has not yet been thoroughly investigated. Understanding the loss mechanisms during lamp life and developing solutions to slow down the degradation process will be critical for making this a choice in four-component phosphor coatings.

A thorough knowledge of the crystal structure and associated electronic structures of the host lattice is crucial for understanding the degradation process of a luminescent material operating inside the harsh environment of a discharge lamp. The crystal structure and associated electronic structure provide the necessary framework to explore various electronic processes including those involving point defects generated in the host lattice. The point defects generated via interaction of the material with plasma and radiation are precursors to colour centres that

*Corresponding author. Fax: +49 6151 16 6015
E-mail address: p.c.schmidt@NOSPAM.pc.chemie.tu-darmstadt.de (P.C. Schmidt).

0022-4596/$ - see front matter © 2005 Elsevier Inc. All rights reserved.
doi:10.1016/j.jssc.2005.12.033

compete with fluorescence of the activator ions. With an aim to understand the degradation mechanism of this phosphor in a fluorescent lamp, we have investigated the crystal structure of this material by X-ray diffraction methods and calculated its electronic structure using a first principles method.

This phosphor was first reported by Murakami et al. [1] as a boron-substituted $Sr_2P_2O_7$ with the composition 2 SrO, 0.84 P_2O_5 and 0.16 B_2O_3. This material was reported to yield tetragonal crystals with $a = 6.92$ Å and $c = 9.51$ Å. The correct chemical formula was deduced by Smets [2] to be $Sr_6B(PO_4)_5$ on the basis of the lattice vectors and comparison to $Sr_2P_2O_7$. Based on synchrotron powder diffraction data, a complete structure model was recently derived and reported [3] around the time this manuscript was being submitted for publication.

In this paper, we report a detailed analysis of the crystal structure of SrBP along with its electronic structure calculated using a first-principles band structure method. In Sections 2 and 3, we describe synthesis of undoped samples of SrBP aimed at producing large crystalline particles. A crystal from these samples was used to obtain a very precise structure model from single-crystal X-ray diffraction data. In addition, thermal expansion between 90 and 1200 K was investigated by synchrotron powder diffraction. In Section 4, the calculated electronic structure of this material using the structural data from the X-ray diffraction measurements is described. Significance of its crystal structure and associated electronic structure is discussed particularly in the context of its performance as host for a luminescent material.

2. Material synthesis

Coarse-grained samples of SrBP were prepared using specially prepared coarser-sized $SrHPO_4$. This precursor was prepared by slowly adding the correct amount of dilute phosphoric acid to a slurry of $SrCO_3$ in water. The resulting $SrHPO_4$ was then assayed to determine its weight loss. This coarser $SrHPO_4$ precursor was then used to prepare a dry mixed blend of the three precursors, $SrHPO_4$, $SrCO_3$ and H_3BO_3 needed to make $Sr_6BP_6O_{20}$. These precursors were mixed by shaking in a plastic bottle using a

Table 1
Structural data for $Sr_6B(PO_4)_5$ from X-ray diffraction measurements

Phase data	
Formula sum	$BO_{20}P_5Sr_6$
Formula weight	1011.38
Crystal system	Tetragonal
Space group	$I\bar{4}c2(120)$
Cell parameters	$a = 9.7895(7)$ Å, $c = 19.032(3)$ Å
Cell ratio	$a/b = 1.0000$, $b/c = 0.5144$, $c/a = 1.9441$
Cell volume	1823.92(34) Å^3
Z	4
Calc. density	3.683 g/cm^3

Table 1 (*continued*)

R_1 (all data, $I > 2\sigma(I)$)	0.0285, 0.0249
wR_2 (all data, $I > 2\sigma(I)$)	0.0633, 0.0641
Pearson code	tI128
Formula type	$NO_5P_6Q_{20}$
Wyckoff sequence	*i7hcb*
Diffractometer	Xcalibur, Oxford-Diffraction
Radiation/wavelength	Mo-$K\alpha$/0.71073 Å
Temperature	303(2) *K*
Crystal size	60 μm × 50 μm × 40 μm
Linear absorption coefficient	17.96/mm
Reflections collected/unique	1234/717
No. of parameters /restraints	74/0
Transmission (min/max)	38.5%/52.7%
Largest difference peak and hole	0.663 and −0.596 eÅ^{-3}

Atomic parameters

Atom	Ox.	Wyck	Site	SOF	x/a	y/b	z/c	U (Å^2)
Sr1		16*i*	1		−0.00242(10)	0.19982(8)	−0.16504(4)	
Sr2		8*h*	2		−0.22145(7)	0.27855(7)	0	
P1		4*b*	−4		0	0	0	
P2		16*i*	1		−0.0214(2)	0.2949(2)	−0.34864(9)	
B1		4*c*	−4		0	1/2	−1/4	
O1		16*i*	1		−0.0778(6)	0.4013(6)	−0.2912(2)	
O2		16*i*	1		0.0270(7)	0.1292(6)	−0.0442(3)	
O3		16*i*	1		0.0055(7)	0.1634(6)	−0.3068(3)	
O4		16*i*	1		−0.1425(6)	0.2762(7)	−0.3949(3)	
O5		16*i*	1		0.1036(6)	0.3534(6)	−0.3835(3)	

Anisotropic displacement parameters (Å^2)

Atom	U_{11}	U_{22}	U_{33}	U_{12}	U_{13}	U_{23}
Sr1	0.0181(5)	0.0081(4)	0.0105(3)	0.0009(4)	0.0007(4)	0.0001(3)
Sr2	0.0117(3)	0.0117(3)	0.0070(4)	−0.0005(4)	0.0005(4)	−0.0005(4)
P1	0.0098(12)	0.0098(12)	0.0070(18)	0.00000	0.00000	0.00000
P2	0.0096(11)	0.0072(11)	0.0091(8)	0.0004(8)	−0.0002(8)	0.0001(8)
B1	0.009(5)	0.009(5)	0.011(8)	0.00000	0.00000	0.00000
O1	0.004(3)	0.011(3)	0.011(2)	−0.001(2)	−0.002(2)	−0.004(2)
O2	0.024(4)	0.015(3)	0.013(3)	−0.006(3)	−0.002(3)	0.005(3)
O3	0.028(4)	0.010(3)	0.012(2)	0.005(3)	0.002(4)	0.001(2)
O4	0.018(3)	0.024(4)	0.018(3)	−0.001(3)	−0.003(3)	−0.009(3)
O5	0.015(3)	0.015(3)	0.020(3)	−0.007(3)	0.012(3)	−0.007(3)

Selected bond distances (Å)

Sr1–O1(#1)	3.194(5)
Sr1–O1(#2)	2.532(6)
Sr1–O2	2.419(5)
Sr1–O3(#1)	2.722(5)
Sr1–O3(#2)	2.558(6)
Sr1–O3(#3)	2.610(7)
Sr1–O4(#1)	2.931(6)
Sr1–O4(#2)	2.966(7)
Sr1–O5	2.559(6)
Sr2–O2(#1)	2.960(7)
Sr2–O2(#2)	2.755(6)
Sr2–O2(#3)	2.960(7)
Sr2–O2(#4)	2.755(6)
Sr2–O4(#1)	2.462(6)
Sr2–O4(#2)	2.462(6)
Sr2–O5(#1)	2.604(5)
Sr2–O5(#2)	2.604(5)

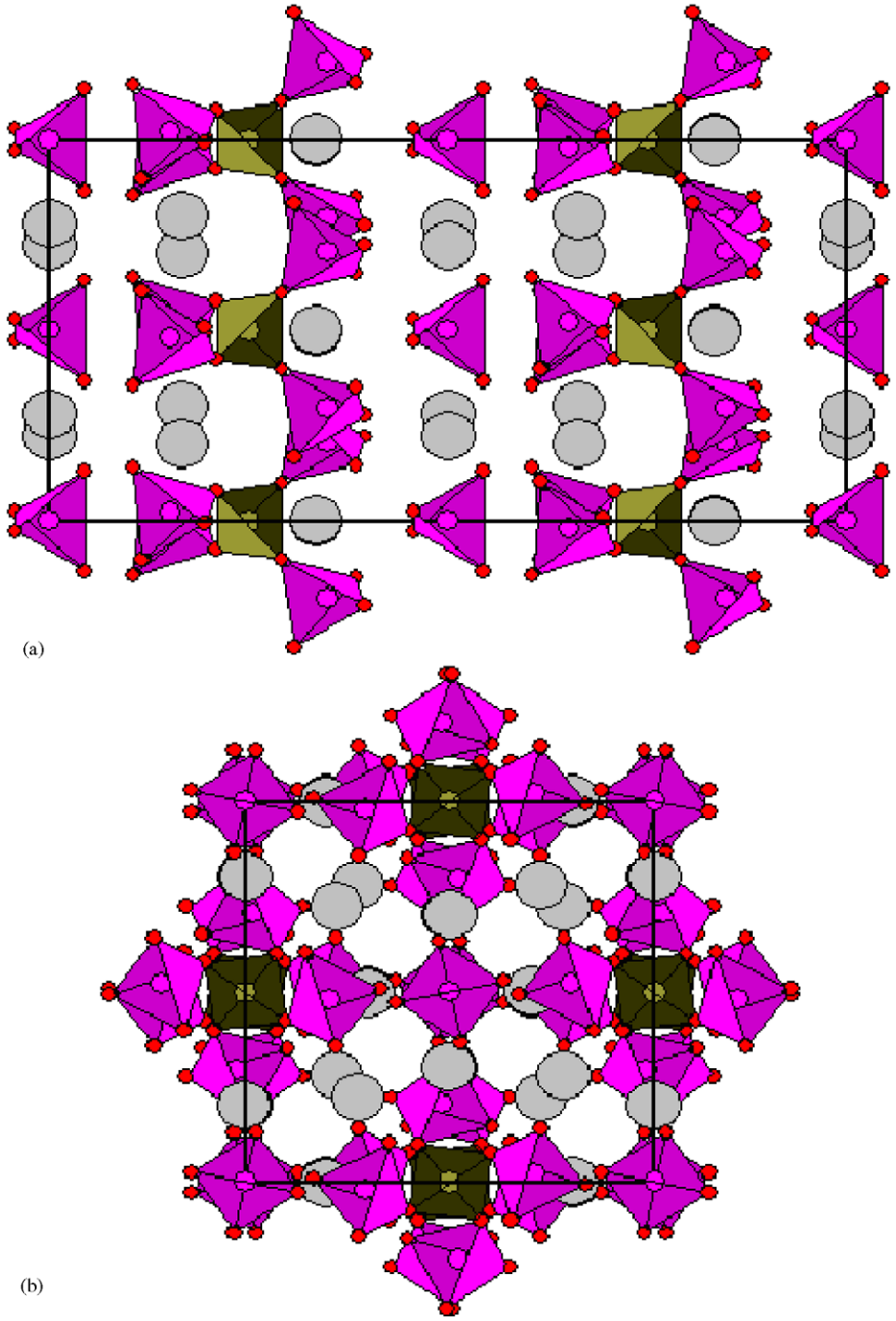

Fig. 1. (a) Crystal structure of $Sr_6B(PO_4)_5$ viewed along [1 0 0] direction. The large spheres correspond to Sr atoms, and the pink and blue tetrahedra to phosphate and borate groups respectively; (b) view along [0 0 1] direction. Note the empty channels.

paint shaker followed by roller mill mixing. The precursors were mixed in proportions of 5.030 mol of $SrHPO_4$, to 0.9700 mol of $SrCO_3$ and 1.050 mol of H_3BO_3. These proportions yield an excess of 5% B and 3% P over the stoichiometric proportions and are needed to account for volatilization losses. Enough of each blend was prepared to yield approximately 300–350 g of material before firing.

These blends were loaded into silica crucibles, covered and fired in a programmable electric furnace. They were heated to a temperature of 1200 °C over 5 h, held at 1200 °C for 5 h then cooled to room temperature over 6 h. Firing weight losses were noted to be slightly greater than the sum of the predicted component weight losses, indicating that the use of excess amounts of boron and phosphorus were justified. After firing, they were mortared and sieved past 150-mesh. The mortared and sieved powder was either milled or tested as is. Fines were removed from some of these blends by elutriation, i.e. suspending the particles and

water, allowing the coarser particles to settle and pouring off the finer particles held in suspension.

3. X-ray diffraction measurements

Diffraction data from a prismatic crystal (size 60 μm × 50 μm × 40 μm) from the phosphor powder samples have been collected with Mo-$K\alpha$ radiation and CCD SAPPHIRE2 detector in φ-scan mode on the Xcalibur system with the ENHANCE-X-ray source option from Oxford Diffraction [4]. A combined empirical absorption correction with frame scaling was applied, using the *SCALE3 ABSPACK* command in CrysalisRed [5]. All observed reflections could be indexed, based on a tetragonal body-centered cell. Altogether, 701 reflections have been considered for the refinement of cell parameters. SHELXS-97 and SHELXL-97 [6] have been used for structure solution and structure refinement, respectively. The optimum structure model is summarized in Table 1 and confirms the previously reported structure, which had been derived from synchrotron powder diffraction data [3].

The crystal structure of SrBP (equivalently $Sr_6(BP_4O_{16})(PO_4)$) is built up of BO_4- and PO_4-tetrahedra, see Figs. 1a and b. The main characteristic BP_4O_{16} unit of five corner-sharing tetrahedra consists of one central BO_4-tetrahedron with local symmetry -4, surrounded by four PO_4-tetrahedra. From the perspective of phosphor chemistry, it is particularly interesting to examine the local environment of the strontium atoms. The divalent europium ions are likely to substitute for these ions in this structure. The strontium atoms, Sr1 and Sr2 occupy two distinct Wyckoff sites 16*i* and 8*h* (see Table 1). Sr1 has nine oxygen neighbors at distances ranging from 2.419 to 3.194 Å. The longest Sr1–O1 distance of 3.194 Å is comparable to that of Sr1–B distance of 3.354 Å. Based on the ionic radii of Sr and O atoms, the Sr–O bond lengths should be in the range of 2.53 Å for six coordination to 2.66 Å for eight coordination. Thus, the range of bond lengths for Sr1 in this crystal is large compared to typical Eu^{3+} coordinations [7]. The second strontium atom is bonded to eight oxygen atoms at distances ranging from 2.462 to 2.960 Å. If one excludes the largest Sr1–O bond length, the range is comparable to that of Sr1. The next nearest neighbor is a phosphorus atom at 3.484 Å. There are no boron atoms in the next coordination shell.

We performed high-temperature powder diffraction with synchrotron radiation at beamline B2 [8] of the Hamburger Synchrotronstrahlungslabor (Germany) in the temperature range from 300 to 1200 K. Monochromatic radiation ($\lambda = 0.50023$ Å) was selected from the primary beam by a Si(1 1 1) double-crystal monochromator. A commercially available furnace from STOE was used for heating the sample in a 0.3 mm diameter quartz capillary. Full-profile Rietveld refinement was applied, based on the structure model from single-crystal diffraction. One common isotropic displacement parameter u_{iso} for all atoms was sufficient in the refinements for good agreement between calculated profiles and observed high-temperature synchrotron powder diffraction data. The mean square-displacement parameter u_{iso} increases linearly with temperature, and the slope is inverse proportional to the harmonic potential parameter D in $E(r) = 1/2\,D\,r^2$. The value $D = 41450(k_B\,K/Å^2)$ is derived from the experimental data.

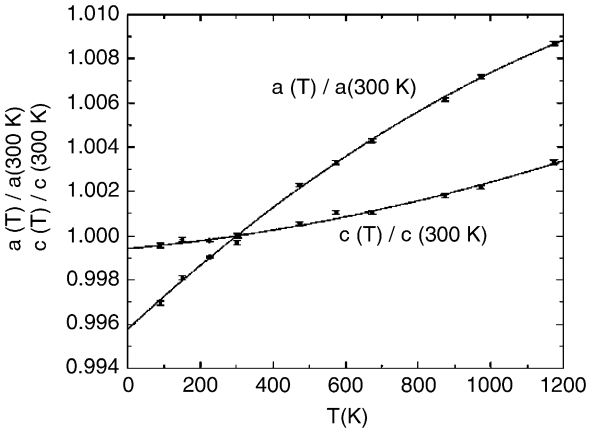

Fig. 2. Relative changes of lattice parameters as a function of temperature, $a(T)/a(300\,K)$ and $c(T)/c(300\,K)$, respectively. The drawn line are polynomial fits of first- and second-order respectively, $a(T)/a(300\,K) = 0.99579 + 1.41782 \times 10^{-5}\,T/K$ and $c(T)/c(300\,K) = 0.99942 + 1.01055 \times 10^{-6}\,T/K + 3.98069 \times 10^{-9}\,T^2/K^2$. The data are normalized to $a(300\,K) = 9.7813$ Å and $c(300\,K) = 19.0091$ Å.

Additional low-temperature data have been collected with Mo-$K\alpha_1$ radiation on a STOE STADIP diffractometer, equipped with a linear position-sensitive detector. The thermal expansion in the low- and high-temperature region is highly anisotropic as shown in Fig. 2 and much more pronounced in the *ab*-plane. A more or less linear behaviour is observed for the *a*-axis in the whole temperature range, but a pronounced flattening below 400 K for the *c*-axis. Lattice parameters between 90 and 1173 K have been determined by full structure Rietveld refinements using the Winplotr software package [9].

4. Electronic structure calculations

We have calculated the electronic band structure of SrBP using the augmented spherical wave (ASW) method [10] in a new scalar-relativistic implementation [11]. This is a density functional (DFT) method based on the atomic sphere approximation with spherically symmetric potentials within the Wigner–Seitz spheres centred at the nuclei. To fill the inter-atomic space in the open crystal structure of SrBP, several empty spheres are inserted. They can be considered as pseudo atoms without nuclei and are assigned a basis set appropriate for describing the electronic distribution within the sphere. They have been found to be useful for modelling the correct shape of the crystal potential within large voids. A sphere geometry optimization (SGO) algorithm [12] is applied to determine the optimal empty sphere positions as well as radii of all spheres automatically. A minimal basis set consisting of

Sr(5*s*,4*p*,4*d*), B(2*s*,2*p*,3*d*), P(3*s*,3*p*,3*d*) and O(2*s*,2*p*,3*d*) atomic functions is used for the present calculation. The v. Barth–Hedin local density approximation (LDA) exchange-correlation potential [13] and a $12 \times 12 \times 12$ k-mesh in the full Brillouin zone are applied.

The ordering of the electronic states of $Sr_6B(PO_4)_5$ are shown in the density of states (DOS) and the partial DOS (PDOS) plots in Fig. 3. The labelling of the ions is the same as in Table 1. The upper valence band edge E_F is chosen to be the zero of the energy scale. The energy peaks of the PDOS below −16 eV are the 2*s*-like states of O and P. Above these bands are the 4*p*-like states of Sr1 and Sr2. The valence states in the energy range of about −10 to 0 eV are predominantly 2*p*-like states of the five different oxygen ions. The lower conduction states between 5 and 8 eV are predominantly Sr 4*d*-like states where the lowest *d*-like states are the d_{yz} states of Sr1. These states are separated by a small band gap at about 6 eV from the other *d*-like states. This can be seen more clearly from the band structure which is shown in Fig. 4. We find a direct optical band gap

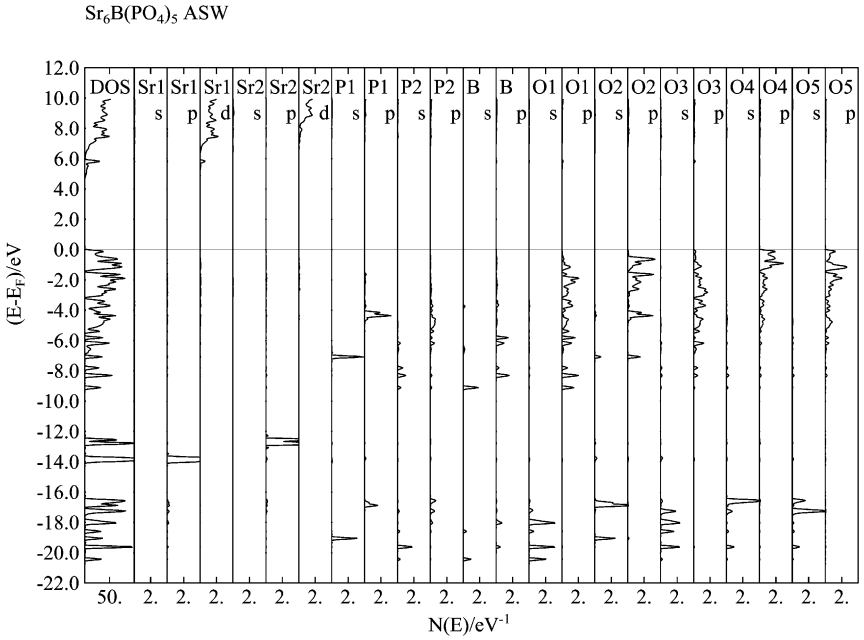

Fig. 3. Density of states (DOS) and partial DOS of *bct* $Sr_6B(PO_4)_5$. The top of the valence bands is the zero of the energy scale. The atomic labels for the partial DOS are the same as in Fig. 1. The *s* and *p* components of the partial DOS are plotted and additionally for Sr the *d* component.

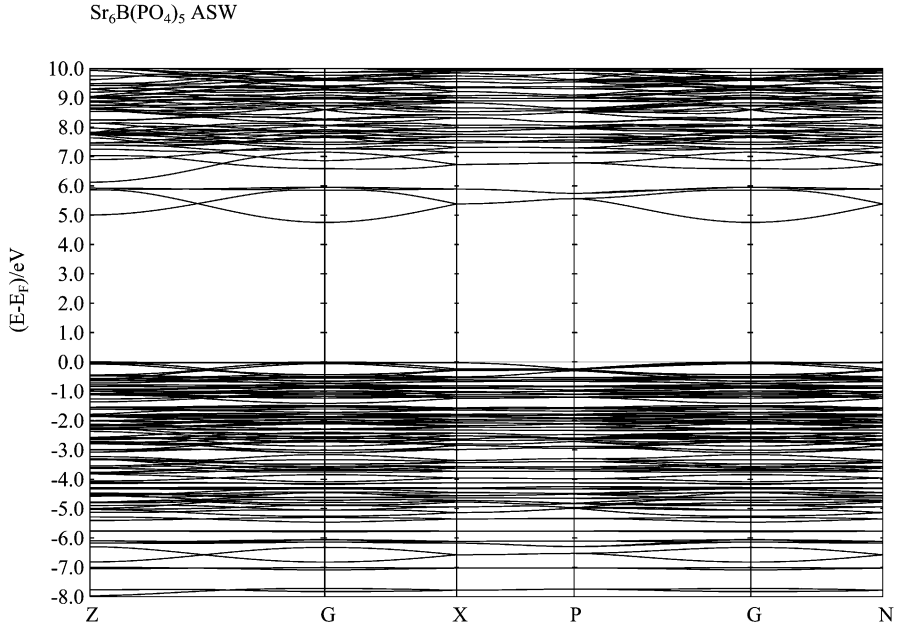

Fig. 4. The band structure of $Sr_6B(PO_4)_5$ along some directions in the *bct* Brillouin zone. The energy scale is the same as in Fig. 2.

at the Γ point of about 5 eV and the mentioned small band gap above the lowest four conduction bands. It is expected that the value of the calculated optical band gap of about 5 eV will be smaller than the experimental one as the LDA underestimates the size of the optical band gap. This material thus belongs to the category of phosphors with large band gap that are usually good hosts for many luminescent ions. The large band gap helps to accommodate both the ground and excited states within the band gap.

5. Conclusion

We have reported the precise crystal structure of SrBP, based on single-crystal X-ray diffraction data, which is the host material for commercially available phosphor types L130/Type 248 phosphor within OSRAM Sylvania. This phosphor is activated by divalent europium ions. It is reasonable to assume that the divalent europium atoms occupy strontium sites substitutionally. Both the sites are highly asymmetric and would have distinctly different crystalline fields. The signature of the multiple sites could be seen in the emission and absorption spectra of the material. It would be interesting to see how both the sites behave with ageing within the lamps. ^{151}Eu Mössbauer measurements are in progress to identify local environment of europium ions in SrBP.

References

[1] K. Murakami, J. Narito, Y. Anzai, H. Itoh, S. Doi, K. Awazu, J. Illum. Eng. Jpn. 3 (1979) 6–11.
[2] B.M.J. Smets, Mater. Chem. Phys. 16 (1987) 283–299.
[3] N. Shin, J. Kim, D. Ahn, K.-S. Sohn, Acta Crystallogr. C 61 (2005) i54.
[4] CrysalisCCD, Data Collection GUI, Version 1.171.26, Oxford Diffraction Poland (2005).
[5] CrysalisRed, CCD Data Reduction GUI, Version 1.171.26, Oxford Diffraction Poland Sp. (2005).
[6] G.M. Sheldrick, SHELX97, Programs for Crystal Structure Analysis, University of Göttingen, Germany, 1997.
[7] R.D. Shannon, Acta Crystallogr. A 32 (1976) 751–767.
[8] M. Knapp, C. Baehtz, H. Ehrenberg, H. Fuess, J. Synchrotron Radiat. 11 (2004) 328.
[9] T. Roisnel, J. Rodriguez-Carvajal, Mater. Sci. Forum 378–381 (2001) 118.
[10] A.R. Williams, J. Kübler, C.D. Gelatt Jr., Phys. Rev. B 19 (1979) 6094.
[11] V. Eyert, Int. J. Quantum Chem. 77 (2000) 1007.
[12] V. Eyert, K.-H. Höck, Phys. Rev. B 57 (1998) 12727.
[13] U.v. Barth, L. Hedin, J. Phys. C 5 (1972) 1629.